

# Fabrication of Targets with Foam Lined Hohlraums

S. Bhandarkar, T. Baumann, N. Alfonso, C. Thomas, K. Baker, A. Moore, C. Larson, D. Bennett, J. Sain, A. Nikroo

August 8, 2017

Fusion Science and Technology

#### Disclaimer

This document was prepared as an account of work sponsored by an agency of the United States government. Neither the United States government nor Lawrence Livermore National Security, LLC, nor any of their employees makes any warranty, expressed or implied, or assumes any legal liability or responsibility for the accuracy, completeness, or usefulness of any information, apparatus, product, or process disclosed, or represents that its use would not infringe privately owned rights. Reference herein to any specific commercial product, process, or service by trade name, trademark, manufacturer, or otherwise does not necessarily constitute or imply its endorsement, recommendation, or favoring by the United States government or Lawrence Livermore National Security, LLC. The views and opinions of authors expressed herein do not necessarily state or reflect those of the United States government or Lawrence Livermore National Security, LLC, and shall not be used for advertising or product endorsement purposes.

# **Fabrication of Low Density Foam Liners in Hohlraums for NIF Targets**

Suhas Bhandarkar\*, Ted Baumann, Noel Alfonso<sup>1</sup>, Cliff Thomas, Kevin Baker, Alastair Moore, Cindy Larson, Don Bennett, John Sain and Abbas Nikroo

\* Corresponding author, <a href="mailto:bhandarkar1@llnl.gov">bhandarkar1@llnl.gov</a>

Lawrence Livermore National Laboratory, P.O. Box 808, Livermore, CA 94550

This work was performed under the auspices of the US Department of energy by Lawrence Livermore National Laboratory under Contract DE-AC52-07NA27344

#### **Abstract**

Low density foam liners are seen as a means to mitigate hohlraum wall motion that can interfere with the inner set of beams that are pointed toward the middle section of the hohlraum. These liners need to meet several requirements, most notably the material choice, maximum allowable solid fraction and thickness, that necessitate development of new processing capabilities. Here, we discuss our strategy and work on fabrication of a tantalum oxide foam liner and its assembly into targets for NIF. In particular, we discuss our approach to finding solutions to the unique challenges that come up in working with such low density materials so as to be able establish a viable platform for production of cryogenic targets for NIF with foam lined hohlraums.

#### Introduction

The core mission of the National Ignition Facility (NIF) is to investigate inertial confinement fusion (ICF) using laser as the primary driver. Incoming light energy is used to generate a high temperature (in the order of 1E8K) and pressure (1E11 bar) environment required for fusion of deuterium-tritium (DT) atoms<sup>1-2</sup>. This extreme environment is created through an implosion of a hollow sphere referred to as an ablator. A highly symmetrical implosion is critical for reaching the desired endpoint. One mode of achieving the implosion is called an 'indirect drive' approach where a cylindrical hohlraum composed of high Z elements is struck by the laser beams to produce an intense bath of X-ray radiation<sup>3-4</sup>. An ~2mm diameter ablator containing the DT fuel at about 19K placed at the center of the hohlraum (Figure 1) can thus be subjected to a more

<sup>&</sup>lt;sup>1</sup> General Atomics

diffuse X-ray flux rather than a series of pointed beams impinging directly on the capsule. This is considered to be one of the main advantages of indirect drive.

In this approach, the performance of the hohlraum in producing a spatially symmetric X-ray drive field is key. At NIF, energy is supplied in the form of two sets of 96 laser beams or as upper and lower beams that enter at either axial end of the hohlraum can through the laser entry hole or LEH. Both the lower and upper beams are further split into inner and outer beams (Figure 1) which differ in their angle of pointing inside the hohlraum.

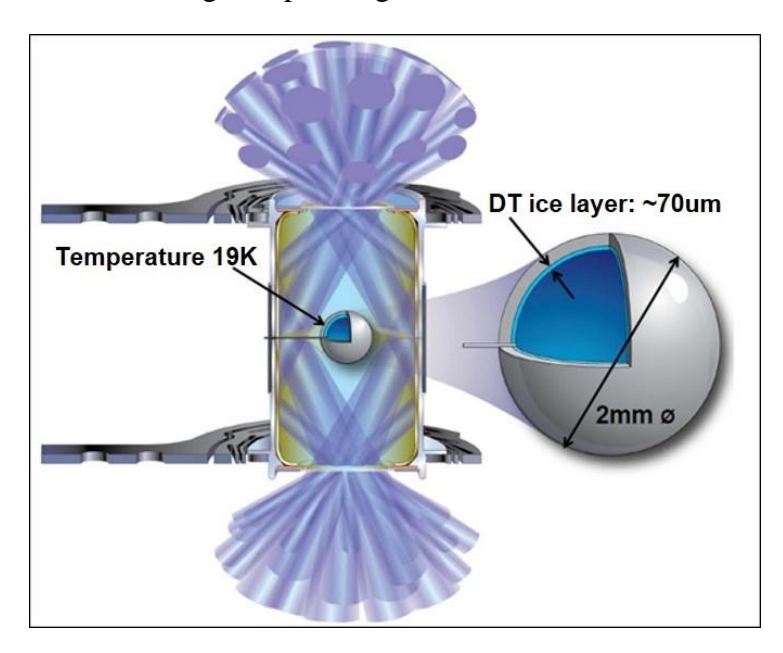


**Figure 1**: Sketch of the core components of the indirect drive target and the splitting of the laser beams into sets of uppers and lowers. Also shown is the relative pointing of the inner and outer beams within each of the sets.

The outer beams impinge on the can closer to the LEH end compared to the inner beams. Outer beams seek to generate the x-rays that drive mostly the polar section of ablator capsule while the inner ones drive mostly the equatorial section. Correctly balancing the energy in the inner and outer beams is crucial to getting a symmetrical drive.

However, interaction of the beams with the hohlraum wall also creates a plume of plasma of the hohlraum material (typically Au with or without U) that moves inward<sup>4</sup>. This plasma field can interfere with the inner beams causing both undesirable back-scatter and refraction. As a result, we can lose energy and suffer from control of the accuracy of beam pointing. This blowoff of the hohlraum material can be arrested using higher tamping gas in the hohlraum, often He, which serves to retard the motion of the plume. However, the plasma generated by the tamping gas itself can itself lead to undesirable laser-plasma interactions (LPI) such as stimulated Raman and Brillouin scattering (SRS and SBS) and cross-beam energy transfer (CBET). This defeats the

purpose of using it in the first place. Indeed, implosions from low fill hohlraums show greater symmetry.

Lining the wall of the hohlraum with a very low density foam could be an effective means of mitigating against the harmful effects of the inward wall motion of the hohlraum while using low tamping gas fills<sup>4-6</sup>. This has a potential of greatly improving the symmetry of the implosion (Figure 2) and hence represents an important advance.

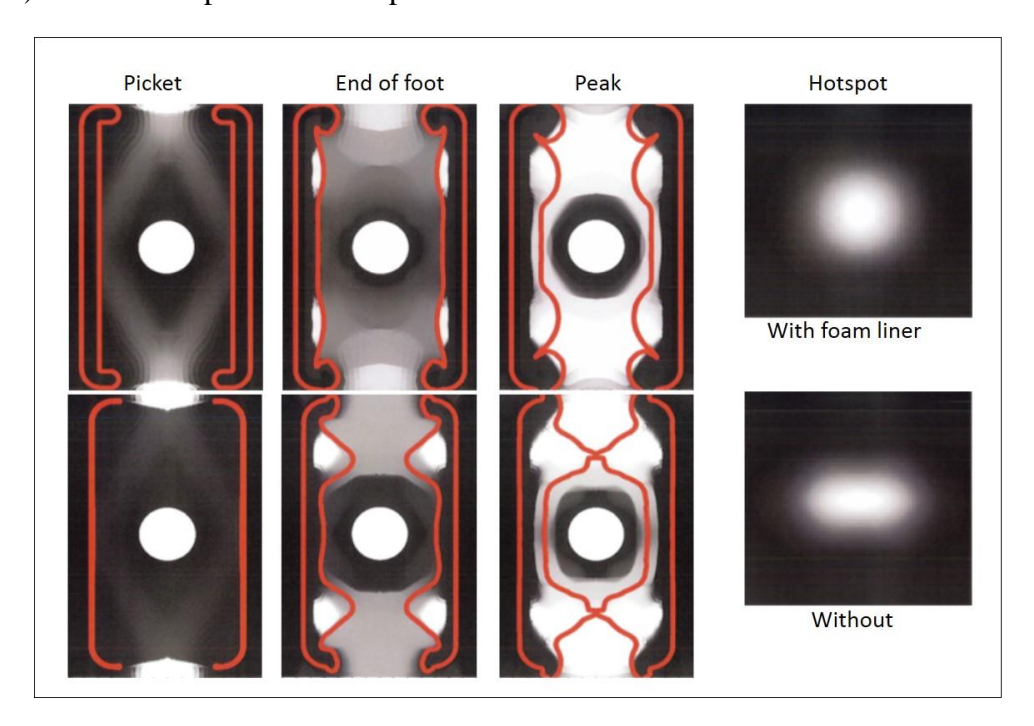


**Figure 2**: Simulation-derived cross-sectional schematic of the motion of the bubble generated by the laser beams striking the hohlraum at different points in time with and without the foam liner. Picket is the earliest part of the laser pulse, foot is middle and peak is last. The lines trace the motion of the hohlraum wall plasma. In the absence of the foam, the plasma fills a significant fraction of the space above and below the capsule which causes asymmetric pointing and affects the roundness of the implosion which is shown by the shape of the hotspot.

In fact, this notion has been around for some time<sup>5</sup> but the renewed interest in the implementation of this approach is only more recent and is spurred by data from NIF shots that calls for a more radical approach for achieving better symmetry of the implosions.

The fabrication of such liners that meet the myriad of physics and target assembly requirements is the crux of this work. Our initial goal has been to ensure that the benefits indicated by simulations of the laser-hohlraum interaction are experimentally verified. Whereas simulations account for the foam as a homogenous material of a certain density, practical liners can quickly diverge from this ideality. For instance, foams can have a variety of different microstructures depending on the process used to make them. The effect of the microstructure would need to be explored experimentally. Likewise, the lower threshold of the density that meets the desired

functionality would be another such experimentally derived result. Hence, our approach was to use the computer codes as a guideline to drive an experimental program of shots whose goal was to evaluate the validity of the concept.

### Requirements for the foam liner

Ideally, the foam would be simply comprised of the same material as the hohlraum, only with a much lower density. The common hohlraum material for ICF targets on NIF is Au, therefore the liner would be made of a Au foam with a density <<200 mg/cc (solid fraction of <<1/100). However, there is no established process for fabrication of a gold foam of this density. This meant that we needed to develop such a process or look for an alternate material that can reach low densities. Keeping the hohlraum X-ray drive in mind, a logical starting material for making the foam would be one that also has a high Z (atomic number > 60). In the long run, further attributes of the foam material could include presence of a low Z component to mitigate for SBS through ion-acoustic damping and incorporation of mid Z components or rare-earth oxide material for suppression of the M band X-rays to minimize the need for a dopant in the low Z capsule. Whereas these ideas provide room for future tweaking of the foam liner composition, our starting point was with the use of a high based Z material.

Furthermore, we set other requirements for the liner to include:

- Density: needs to be in the order of 20 mg/cc or lower. Simulations suggest such a low density is essential for optimal performance but, as mentioned earlier, the impact of density on wall motion mitigation is one of our primary experimental goals. We would like the liner to go no lower in density than is shown to be necessary. This is because the handling yield can be expected to be lower at lower densities.
- Location: needs to include at least the region struck by the outer beams on both hohlraum halves. The foam also may extend beyond depending on the purpose of a specific target or technique used to fabricate it.
- Thickness: needs to be high enough that it avoids burn-through so as to avoid premature exposure of the solid hohlraum wall to the laser pulse. General rule of thumb would be to use a rho\*t (density multiplied by thickness) of ~5um-g/cc. So, for a density of 10 mg/cc, the thickness would be ~500um.
- Pore size: needs to be small. Initial requirement is that the maximum line of sight pore be <1% of the thickness.
- Density variability: needs to be <10% around the entire liner

We see these as starting stipulations that get refined as shot results yield more information on each of these requirements and redistribute their relative importance.

# Fabrication and characterization of Tantala aerogel liner made using machining

Several methods are being developed for the fabrication of foam liners. They can be broadly separated into two categories: one that uses casting from a solution or a dispersion, and another that uses a removable template upon which a small amount of the foam material is deposited to achieve the expected density. All the work described here will be on the use of tantalum oxide (Ta<sub>2</sub>O<sub>5</sub>) aerogel as the foam material. The choice of this starting point was based on the fact that there was an existing process for making Ta<sub>2</sub>O<sub>5</sub> aerogels which grants us the ability to launch quickly into making shot targets. Additionally, Ta<sub>2</sub>O<sub>5</sub> is a desirable material for the foam<sup>7</sup> for two reasons: it has significant fraction of a high Z element (Ta) which addresses the X-ray drive requirement but also has some low Z oxygen that potentially can lower SBS. Being able to make the foam quickly also allows us to develop all the modifications to the assembly steps for a foam lined hohlraum based cryogenic target. As stated above, other ideas to make the initial foam have been conceived by different groups of researchers have. These diverse approaches, which are at varying levels of maturity of development, will not be described here but likely later in other publications. Our intent in nurturing alternate methods is to ensure that we have multiple options to bring to bear if we uncover unforeseen susceptibilities with our baseline process during assembly and fielding of the integrated target.

In a nutshell, the Ta<sub>2</sub>O<sub>5</sub> aerogel process involves making a solution that gels<sup>8-9</sup>. Removal of the entrapped liquids supercritically avoids capillary forces and preserves the initial network of the gel with no shrinkage per se. The resultant product is called an aerogel. Density control is achieved by changing the concentration of the active ingredients. This technique has been used for making other components for ICF shot targets but typical densities have been greater than 100 mg/cc. Our challenge here was twofold: to cast at lower density and to form it into a liner. In principle, molding the aerogel into a foam liner directly inside a hohlraum half with a smaller but shape-matched mandrel to define the liner thickness is an obvious idea but the removal of the mandrel is non-trivial. The fragility of the foam makes any stiction of the foam to mandrel a mode for catastrophic failure.

As mentioned before, the foam does not need to line the entire inside of the hohlraum but primarily the region where the outer beams hit the hohlraum. Thus, our starting-point design was to have a band of foam that covers a portion of the barrel section of the hohlraum as seen in Figure 3.

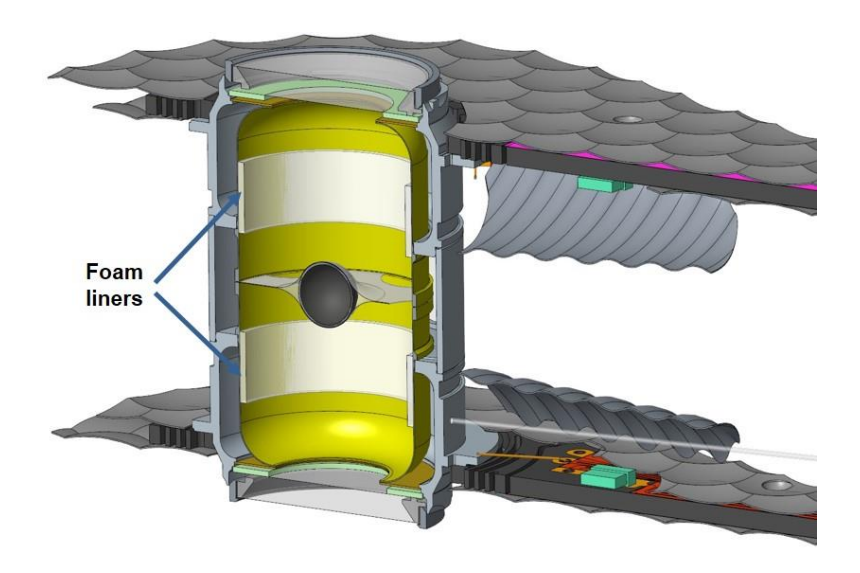


**Figure 3**: Cut-out cross-section of a typical cryogenic target for NIF showing the minimum locations of the foam liners.

This design with a cylindrically symmetric shape allows us to consider machining the foam, albeit done by highly experienced specialists, to define the inner core of the liner. Here is how it was done, with the steps shown in Figure 4.

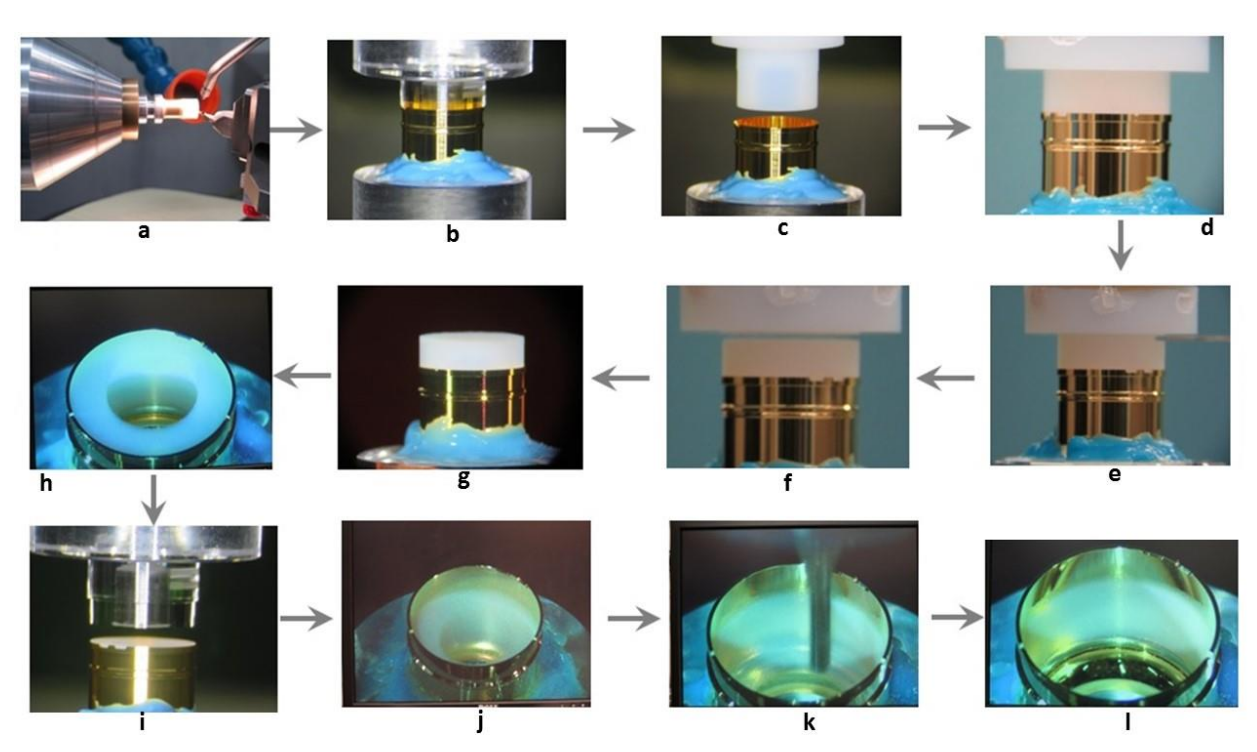


**Figure 4:** Progression of the steps for machining a foam liner: a) Preparatory machining of foam into a cylindrical billet with the starting hole in the center on a lathe b). Potting of the hohlraum onto a post using a removable adhesive c) Aligning the billet machined in step a to the potted hohlraum d) partial insertion of the billet into the hohlraum e) side view of the cutting of the

foam billet using a spinning wire f) separation of the billet from its holder upon completion of the cutting g) side of the foam in the hohlraum ready for further insertion h) top view of the billet flush with the hohlraum waist i) customized pusher readying for insertion of the billet to the right location within the hohlraum j) billet in its final resting place inside the hohlraum k) milling of the inner wall of the billet to achieve the right liner thickness l) final part

A billet of 90 mg/cc tantala aerogel was first cast into a cylinder of diameter greater than inner diameter of the hohlraum. This billet was then turned on a lathe such that its outer diameter was about 20um greater than the hohlraum diameter. Additionally, the center was bored out so as to provide a starting hole for the final machining step described below. The billet was then pushed into the hohlraum such that the foam would be under slight compression because of the mismatch in hohlraum and billet diameters. Once inside the hohlraum, the billet was parted from its holder using a thin spinning wire as a precision cutting tool. Once completely separated, the cylinder of foam was slowly pushed using a custom machined post to its final resting place. Finally, the inside of the foam was milled to obtain the right liner thickness. The resultant final foam lined hohlraum is shown in Figure 5.

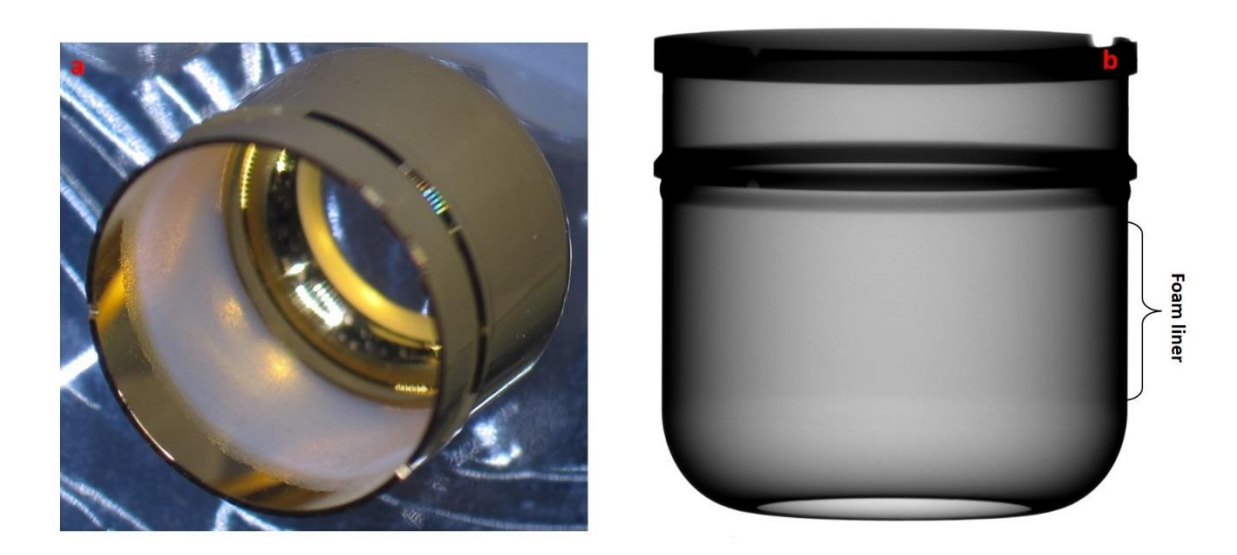


**Figure 5**: a) Optical image of a machined foam lined Au hohlraum half after cryogenic cycling. In this case, the nominal inner diameter of the hohlraum was 5.4mm and length was 5.06mm. Thickness of the 90mg/cc foam liner was 200um and its length was 2.5mm. b) X-ray transmission image where the high opacity of tantala makes the liner faintly visible through the 30um of Au wall of the hohlraum, a technique that offers a means of verification of the liner.

In fact, this image of the hohlraum was taken after it was thermally cycled twice between room temperature and 10K to simulate the temperature range that the final target would see. Even though contraction of tantala is less than that of the surrounding Au, resulting in a slight compressive (not tensile) stress on the foam, we wanted to ensure that there was no cryogenic

degradation of the liner. Indeed, none was seen in all four out four hohlraums tested this way. We extracted a small piece of the liner from a spare hohlraum and characterized it with X-ray tomography using a Zeiss Xradia 510 Versa system (Figure 6). Based on these results (Figure 5 and 6), we see X-ray imaging as an excellent characterization technique both for surface roughness, and bulk homogeneity (discussed later in the paper) of foam liners.

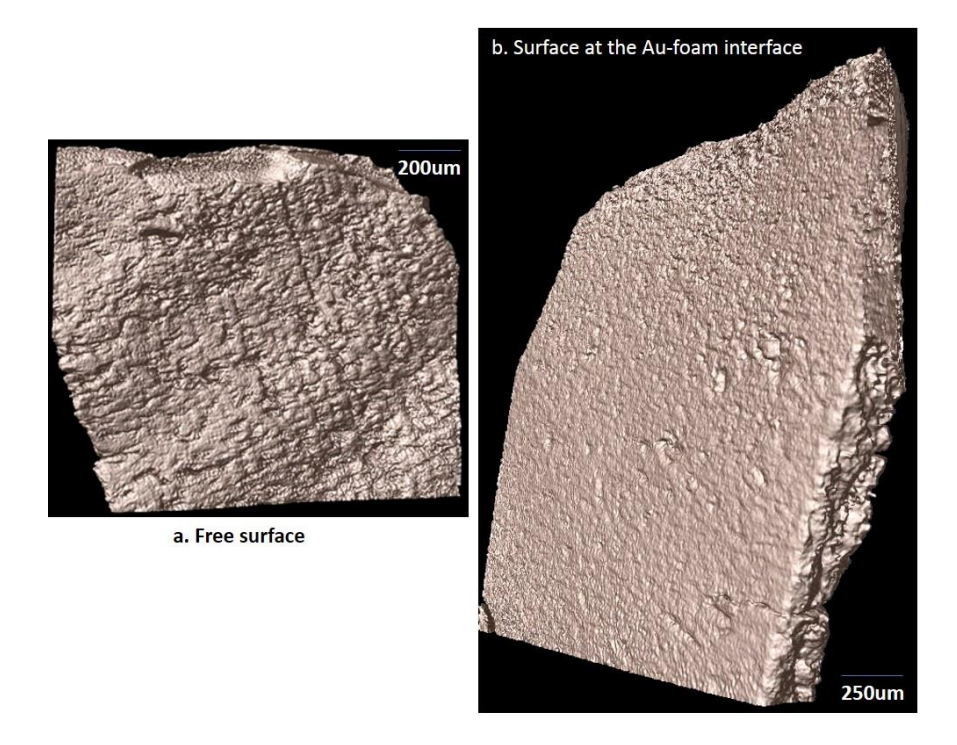


**Figure 6**: Images from X-ray tomography of the inner surface (a) and the surface at the Au wall (b) of the liner of the kind seen in Figure 5. Surface undulations from milling are clearly seen in image a.

We made several such lined hohlraums using this process using foam density of 90mg/cc which allowed us to move ahead with the fabrication of a full-fledged target for a cryogenic shot on NIF. However, we found that it was too difficult to do the milling operation on tantala foams with densities less than 55 mg/cc. The foam tended to smear rather than sever as the cutting tool went across it. This represents a major limitation of this technique.

The target type that was built was the so-called Symmetry Capsule or SymCap, which was meant to provide information on the implosion symmetry and back scatter without generating high yield of neutrons. Data from the shot (N160405) indicated promise for this approach: the peak X-ray flux was within about 7% of that from a Au hohlraum, laser coupling was 99%, and hard X-rays (>1.8keV) were reduced by a factor of about 1.8. Additionally, analysis of the self-emission suggested reduction in wall motion, though a definitive confirmation would need more direct measurements. These results indicated that liners could indeed improve the performance

of the hohlraum. The hotspot, however, was seen to be somewhat pancake-shaped with a significant structure (Figure 7) that implied a break-up of the ablator during the implosion.

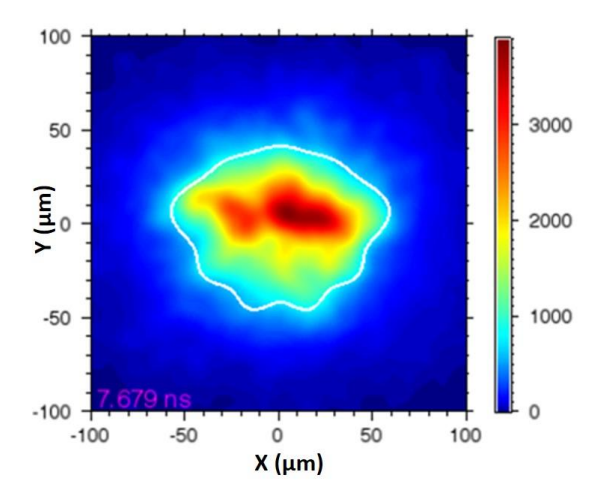


**Figure 7**: Uneven nature of the hot spot at 7.7ns into the implosion

One possible reason for the jagged profile of the hotspot would be the presence of foreign particles on the capsule surface. Since the capsule was known to be largely free of any offending particles before being assembled into the final target, this would need to happen from within the hohlraum. Given the processing pathway for the liner, it wouldn't be unreasonable to expect some debris on the walls of the liner on the hohlraum.

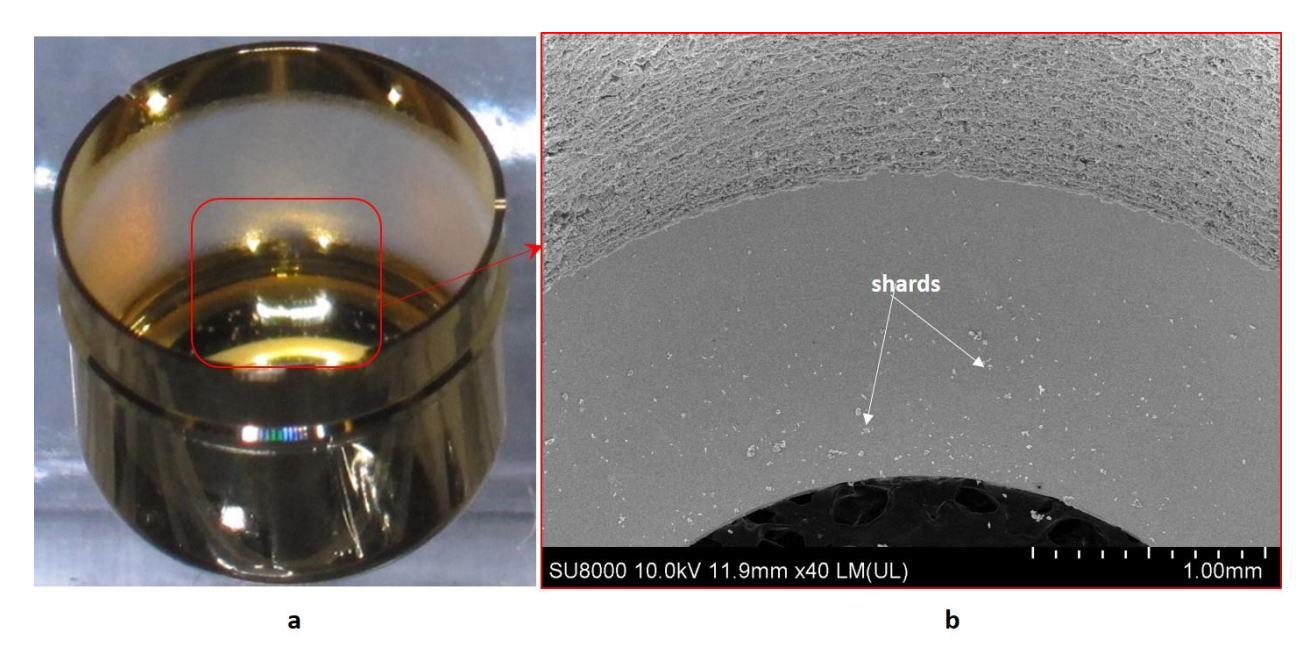


**Figure 8**: a) Optical image of the foam lined hohlraum where shards and debris are clearly seen on the LEH section of the hohlraum b) SEM image of the section of interest confirm the same

Figure 8 shows images of a foam lined hohlraum where particles are readily seen on the LEH end of the hohlraum. But presence of shards does not necessarily mean that they would fall onto the capsule as small particles of foam attached to surfaces often tend to stay put. Surface and electrostatic forces can be strong enough to overcome gravitational pull on a lightweight material. In addition, once the target is assembled, it is customary to handle it gently, primarily to safeguard against impact forces that can jostle the capsule held between two membranes that are less than 50nm thick. So, it wouldn't be a certainty that any particle would come from the foam, despite their presence. But there was one source of excitation that was a bigger concernnamely the vibration imposed by the cryostat. For a cryogenic shot, this can last at least 12 hours.

To test this, we devised a simple way to visualize the particles coming off the liner after it experiences the vibration of the cryostat. We attached a 45nm tent membrane to the waist of the same foam lined hohlraum seen in Figure 5, inspected the membrane surface thoroughly to make sure that it was particle-free to start and then did the same after 30 min of vibration on the cryostat. Figure 9 shows the result from this test, where a large number of particles are clearly seen on the membrane.

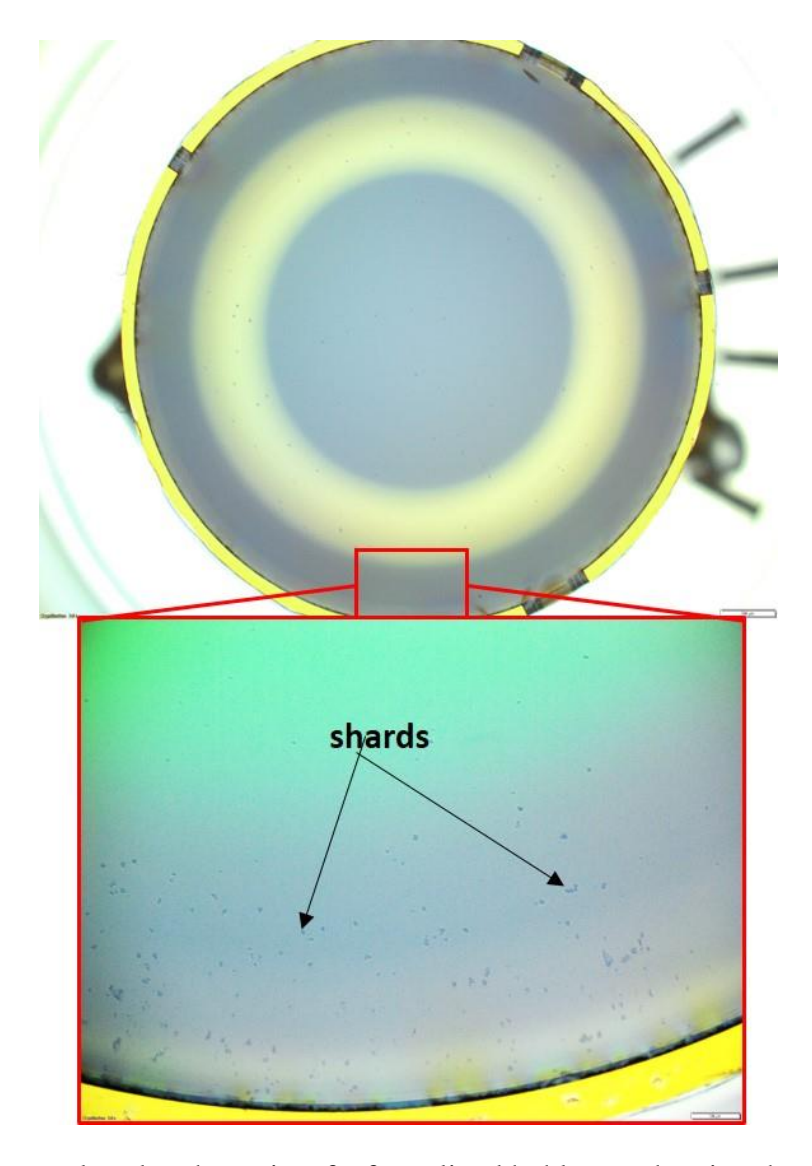


**Figure 9**: Membrane placed at the waist of a foam lined hohlraum showing the accumulation of the particles upon 30 minutes of vibration on the cryostat that's used for cooling NIF targets.

Though almost all of these were located closer to the hohlraum wall than the capsule surface, it still raised the specter of contamination from within the target. Since the foam lined hohlraums used in the Symcap target were machined identically as the one used for the test, it is entirely possible that tantala shards fell on the capsule surface and led to the jetting of the ablator into the hotspot during implosion.

## Foam lined rings as inserts into the hohlraum

One possible source for these particles is the curved LEH region of the hohlraum, where shards are clearly seen (Figure 8). To circumvent this, we designed a slightly modified configuration for the foam lined hohlraums. In this concept, we had a Au ring (in general, the ring would be

comprised of the same material as the hohlraum) which would be lined with the foam. This lined ring would then be assembled into the hohlraum using customized manipulators and glued in place through a small hole in the hohlraum. This obviates collector zones such as the cup-like LEH region but adequately meets the physics need of have a band of foam liner located within the hohlraum barrel. Figure 10, shows a machined liner within a Au ring made using the same method shown in Figure 4.

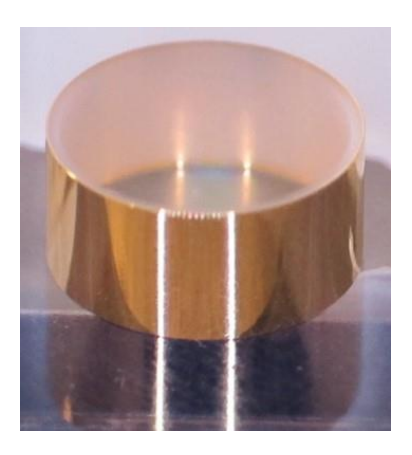
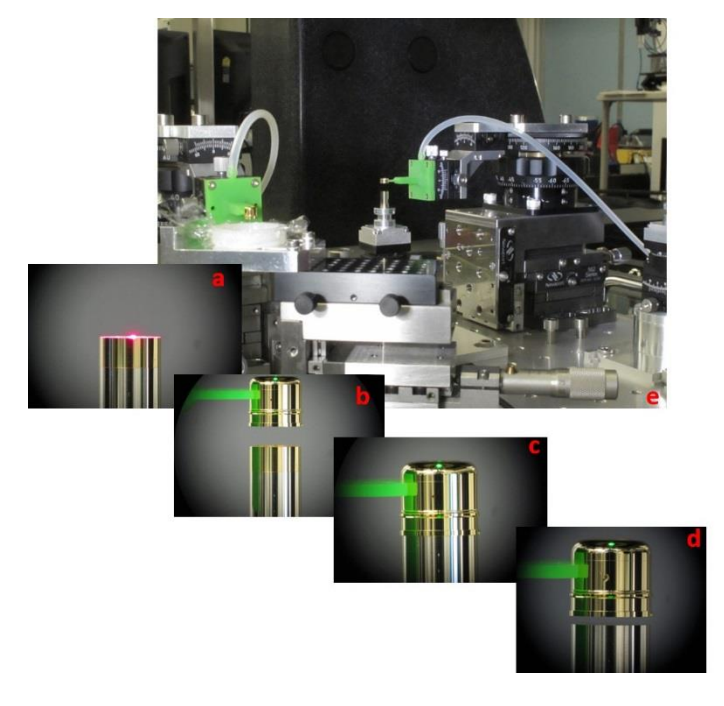
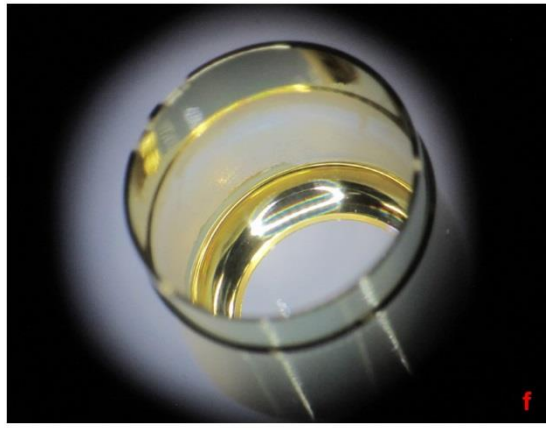


Figure 10: Machined foam lined ring. Liner is 200um thick, comprised of 55 mg/cc tantala

The ring was designed to be 16um smaller in its outer diameter than the inner diameter of the hohlraum so that it readily slides inside the hohlraum. We want to emphasize here that a freestanding foam liner at the thickness (200-500  $\mu$ m) and densities (<20mg/cc) of interest is too fragile for handling. So the ring plays the role of a vital support structure. Figure 11 shows the steps for inserting the ring into the hohlraum.

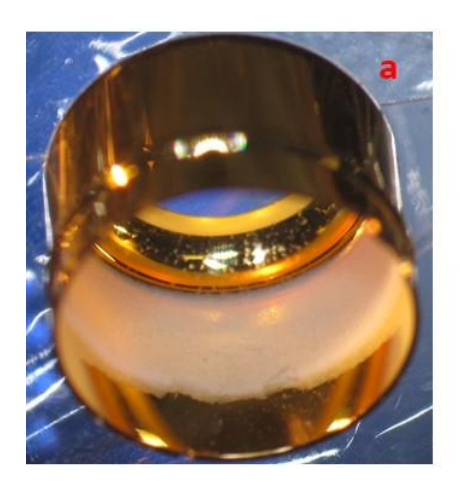




**Figure 11**: Progression of steps to secure the foam lined ring inside the hohlraum. a) Foam lined ring of the type seen in Figure 10 placed on top a custom design post b) Hohlraum, held by a C-shaped vacuum chuck, is lowered over the ring c) hohlraum lowered to a point where the ring is at the appropriate location inside. Note that the hohlraum needs to traverse a portion of the post as well d) Ring is tacked to the hohlraum through a small (250um) hole in the hohlraum using a UV-cured adhesive that can sustain cryogenic cooldown process and the assembly is lifted out e) the micromanipulator system that does tasks a-d f) final part

The ring was placed on a metal post whose outer diameter was in between the outer diameter of the foam lined ring and the inner diameter of the hohlraum. That way, the ring sat freely on top of the post and the hohlraum, held using a vacuum chuck, was slowly lowered using a 3-axis micromanipulator system onto the ring from above. Once the ring was at the right location inside the hohlraum, it was glued in place. As we found earlier, cryogenic cycling of this lined ring showed no detrimental effects. However, under vibration, we found that the lined rings still shed just as many particles as a lined hohlraum. Ostensibly, the loose particles that disperse during this test are located more on the surface of the machined liner than the hohlraum surface.

A second issue that arose when dealing with the inserted foam based approach was the propensity for the liner to slip and move during handling (Figure 12), despite the initial state of compression provided by the deliberate oversizing of the foam billet diameter.



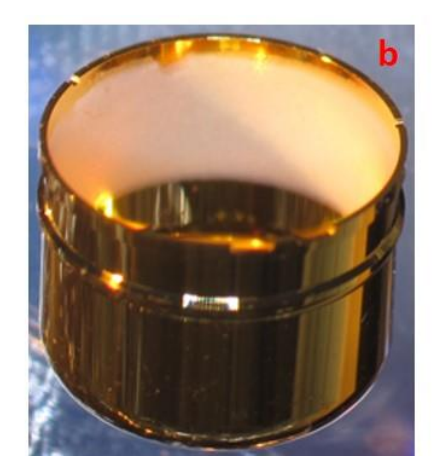


**Figure 12**: a) Machined foam liner in the hohlraum as made b) the same hohlraum 7 weeks after, where the liner is slipped out from its original location. The duration of the time for this occurrence was variable.

About 75% of the parts made this way ended up slipping out of place, in many cases after several weeks of storage in a dry environment and going through multiple handling and characterization without any problems. Presumably, the foam shrinks enough with time that it loses the compressive retaining force. While this issue could ultimately be resolved through refinements of design and handling protocols, the particle shedding problem, coupled with the lower limit on density, effectively ended the prospects of using machined liners for further targets.

#### Laser ablation approach

Nonetheless, these experiments had proved the viability of using of an intermediary ring as the substrate for supporting the liner. One key attribute of this approach is the gain of axial symmetry when the liner is being formed. This makes possible consideration of alternate methods for forming the liner, in particular laser ablation, which greatly raises the potential of overcoming the above problems. Firstly, there is no anticipated lower limit of foam density when using laser cutting. Secondly, there is no mechanical cutting and abrasion action, so the debris problem could be expected to be minimized. Lastly, by casting the foam inside the Au ring rather than inserting it, we could expect to overcome the slippage issue.

This begged the question as to whether the as-cast tantala foam develops good adhesion to the bare Au surface. If needed, one could conceive of enhancing the interfacial adhesion strength by the Au surface with a thin (say 10nm) film of an oxide such as alumina or even tantala, deposited using a process such as atomic layer deposition (ALD). The affinity for an oxide to bond another is much higher due to surface hydroxyls but the question is one of necessity of this step. To quickly probe the degree of bonding, we cast a foam layer on a flat Au substrate as well as an oxide surface and tested them both against nominal impulses seen during the target handling steps. Both samples showed no evidence of delamination due the stresses during testing. Based on this, we proceeded with casting the foam directly inside an uncoated Au ring and avoiding the needless burden of any extra processing steps.

Casting was done by placing the Au ring within a thicker steel ring with a bigger diameter but of exactly the same height (Figure 13a). These rings were then sandwiched between two quartz plates and placed in a separate container which was filled with the sol. The resultant aerogel thus encased the entire assembly. Using a fine brush, the excess foam was carefully removed to excavate the foam filled Au ring. The laser cutting was done using a 266nm frequency quadrupled YAG nanosecond laser (Avia). The beam was focused at the center height of the ring and cutting was done using a computer controlled motion system that allowed cutting to an exact diameter. The laser had a beam diameter of about 20um at the focal point and a focal distance of about 50mm. Pulse repetition rate was 1kHz. We used the lowest power that ablated the foam, which turned out to be 10mW, and a translation speed of 1.67mm/s. We denote this as our baseline process.

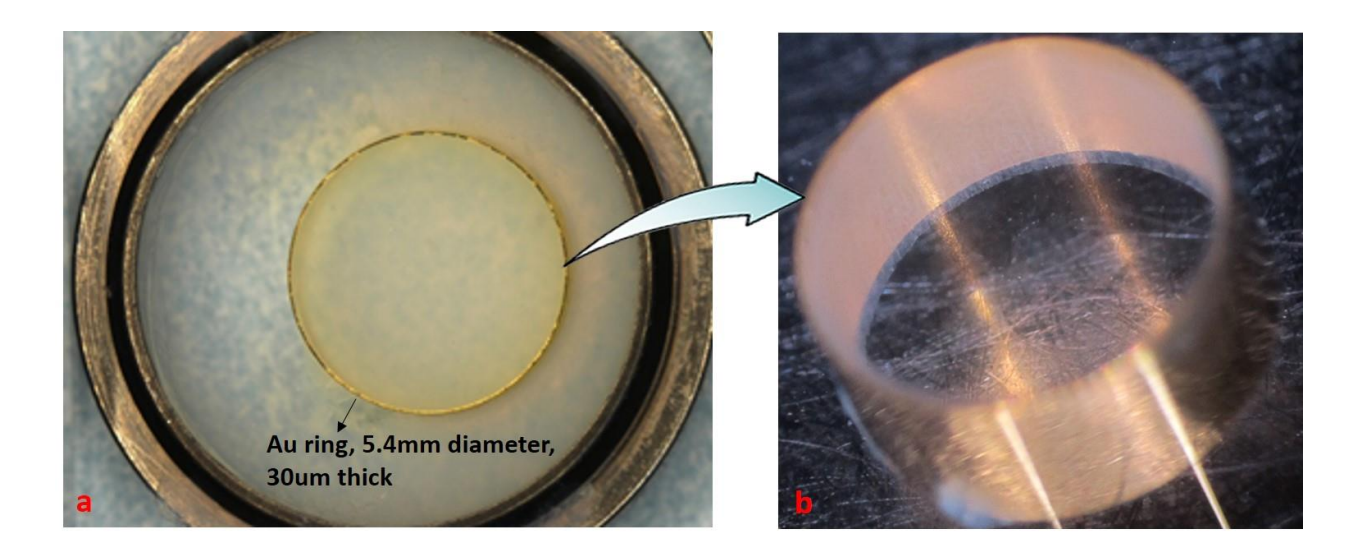


**Figure 13**: a) The configuration for casting a foam filled ring: a thicker outer steel ring of equal length provides reinforcement for the Au ring. This results in foam both inside and outside the Au ring, necessitating the careful extraction of the Au ring before or after laser cutting. b) laser cut foam lined ring with a 200um thick, 20mg/cc tantala foam using the baseline process

Figure 13b shows the image of a ring cut in this manner. For densities under 100 mg/cc, the core was completely detached in 2 passes. In a repeat of the experiment described earlier, we shook the ring in a cryostat with an attached membrane to catch any falling particles and found that there were on average only 5 particles seen, a drastic improvement from the tens of particles that we saw with the machined liners. These were all located very close to the waist of the hohlraum. While the number on any given target will be stochastic, this tells us that there is only a small chance that these particles would land on or near the capsule which represents a significant mitigation of the falling debris problem. Our goal, of course, is to continue to improve the process such that we have high confidence in keeping particles off the capsule. This result underlines the promise of this technique in being able to meet this difficult goal. Furthermore, cooling the lined rings down to 18K caused no degradation of the liner, with no evidence of delamination or slippage.

The surface topography of the inner laser-cut surface for a 20mg/cc is seen in more detail in Figure 14.

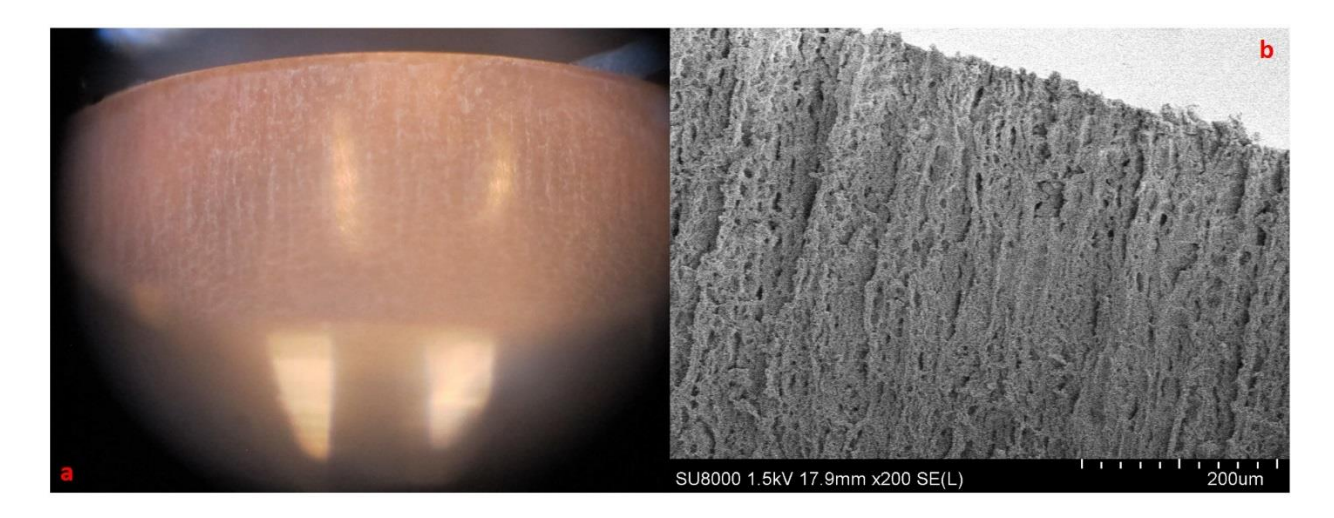


**Figure 14**: a) Optical micrograph of a 20mg/cc laser cut ring showing the vertical striations that are characteristic of the baseline laser cutting process b) SEM micrograph of a surface cut the same way, though not inside the Au ring. In this image, surface flaws such as cavities and large pores are readily visible

It is far from smooth, with numerous cavities and fissures. Additionally, vertical striations can be seen both in the optical and the SEM micrographs. Neither of these two features are severe enough to be unacceptable for early shots. But the foam lined rings showed a tendency to chip, especially at the axial end where it would come in contact with the surface on which it was resting. When the chipping was large enough to affect the region that is struck by the laser beams, the ring was unacceptable. Interestingly, chipping was only seen when the liner was touched, but not when it was shaken or vibrated. Based on microscopic evidence (Figure 15), we inferred that the multiple fissures on the surface likely act as crack-initiation sites.

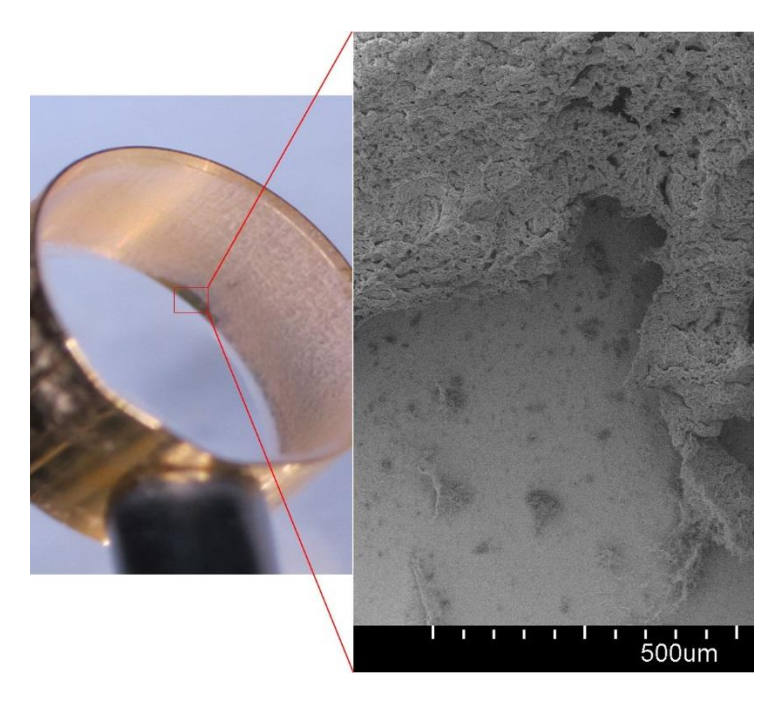


**Figure 15**: Chips spall off the laser cut liner. As seen in the magnified SEM micrograph, each of these chips follow a track defined by a network of surface flaws.

When these sites are close enough to each other to be linked and thus define a weak domain, forces from the scraping of the ring against a surface, however light, created the risk of propagation of cracks that track the domain boundary causing spalling. Because there was no case of the liner sliding as a unit in any of the about 70 such rings we fabricated, yield was essentially a function of the propensity to chip. One mitigation for this was to design a v-block type of container so that the ring is always lying on its side and contact between the exposed liner at the axial ends of the rings and an external surface is avoided. But for greater overall robustness, we sought to develop the laser cutting process further to have micro-crack free surfaces.

# Optimization of the laser cutting process

There are several parameters that can be optimized in a laser cutting process which conventionally leads to a large matrix of possible experiments. Laser ablation based machining is now a mainstream process especially for thin substrate but they are commonly full-density materials such as plastics, metals, and ceramics<sup>10-11</sup>. There are only a few examples in literature of the use laser to shape these very low density aerogels, particularly ceramic aerogels<sup>11-13</sup> and none focused on surface quality. This meant that we needed to do our own investigation, while being mindful of the danger of ballooning the study into an unattainable matrix. Through a series of comparative micrographs below, we show the effect of some of the major parameters involved in laser cutting. In almost all the cases, the cuts were made in an aerogel billet of the

same length as out typical ring (2.5mm long) but cast within a larger stainless ring without the Au ring. Hence these are surrogate cuts that could be metal coated for electron microscopy without wasting the specially manufactured Au rings.

# Effect of foam density:

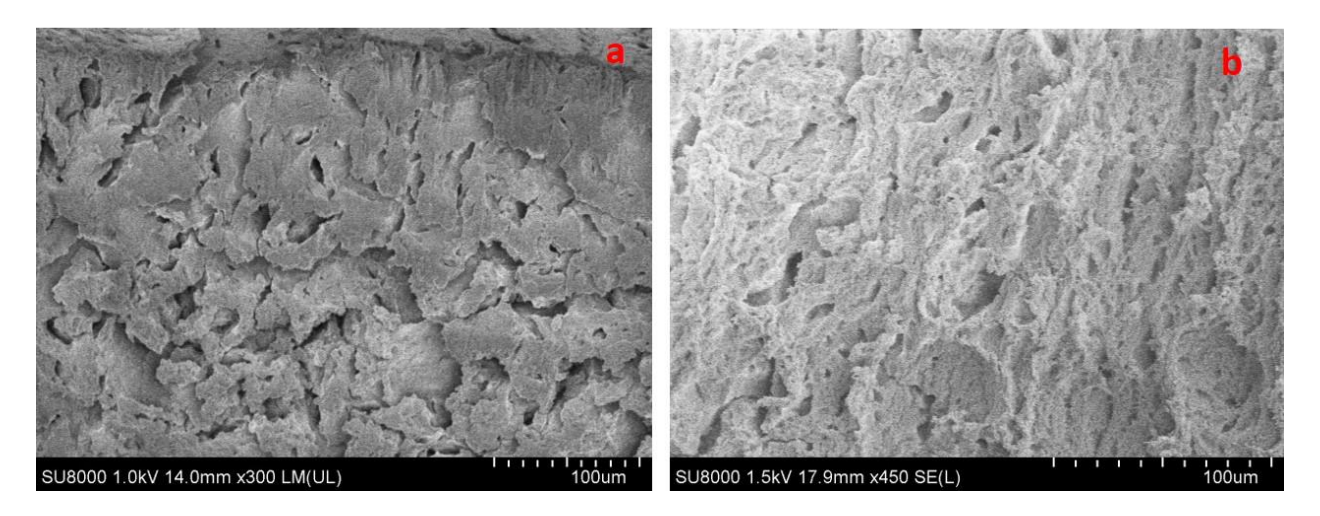


**Figure 16**: Surface features seen in a 45 mg/cc (a) and 20 mg/cc (b) cut using the baseline laser ablation process. Both show a cavernous topography. The smooth surface in between the cavities in (a) is symptomatic of surface melting.

In Figure 16, we compare the surfaces seen for two different densities, 45 mg/cc and 20 mg/cc cut using the baseline process. Both surfaces are heavily pockmarked with multiple cavities where the ablation process has caused portion of the aerogel to be ejected from the surface. Ablation is a process where the transient temperature in the immediate laser-substrate interaction zone reaches levels high enough to vaporize the material being cut<sup>14</sup>. Being a brittle aerogel of a ceramic material, this surface structure may be accounted for by the following mechanism: proximity of set of small flaws within the matrix of the gel create weak domains that are prone to being ejected due to temperature and pressure fluctuations that occur during the ablation process.

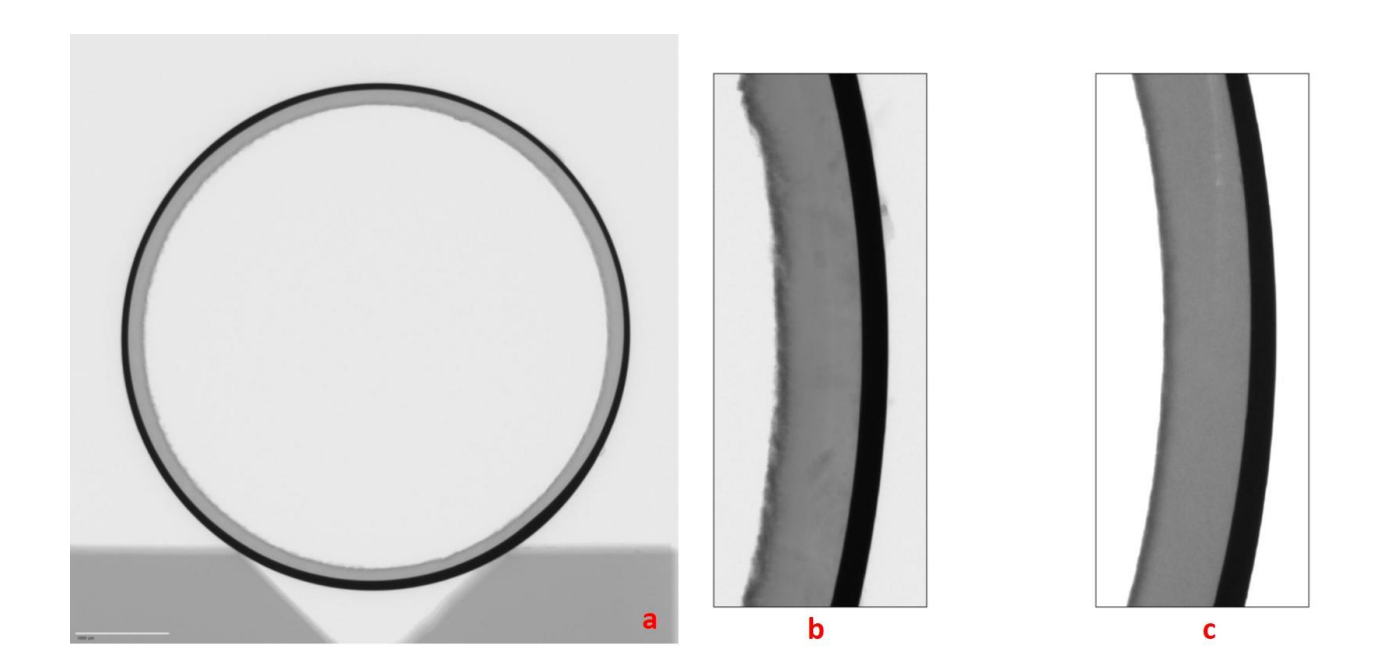


**Figure 17**: a) Axial X-ray transmission image of a 20 mg/cc foam lined ring showing the uniformity of liner thickness. Here the variation was  $\pm$  6um, which was typical. b) Magnified image of the laser cut liner showing a darker and rougher inner surface compared to c) the conventionally machined liner, where the darker band is smaller and more uniform.

The glazed look seen in Figure 16a in the case of the 45mg/cc suggests a skin of molten material, which is almost non-existent in the 20mg/cc sample. Figure 17 shows a X-ray radiograph of the foam with a machined liner for comparison. Both showed low variability in layer thickness circumferentially. One striking difference though is that the inner surface of the laser cut liner has a dark band which is noticeably wider, also hinting at densification due to the laser action. Ablation temperature are known to be very high locally, well over the melting point of even a refractory material such as tantala. So, it is conceivable that the heat transmitted during the ablation process into the remaining foam layer melts some of the surface. To evaluate this further, we fractured a section of the liner and examined the junction under an electron microscope. This is shown in Figure 18.

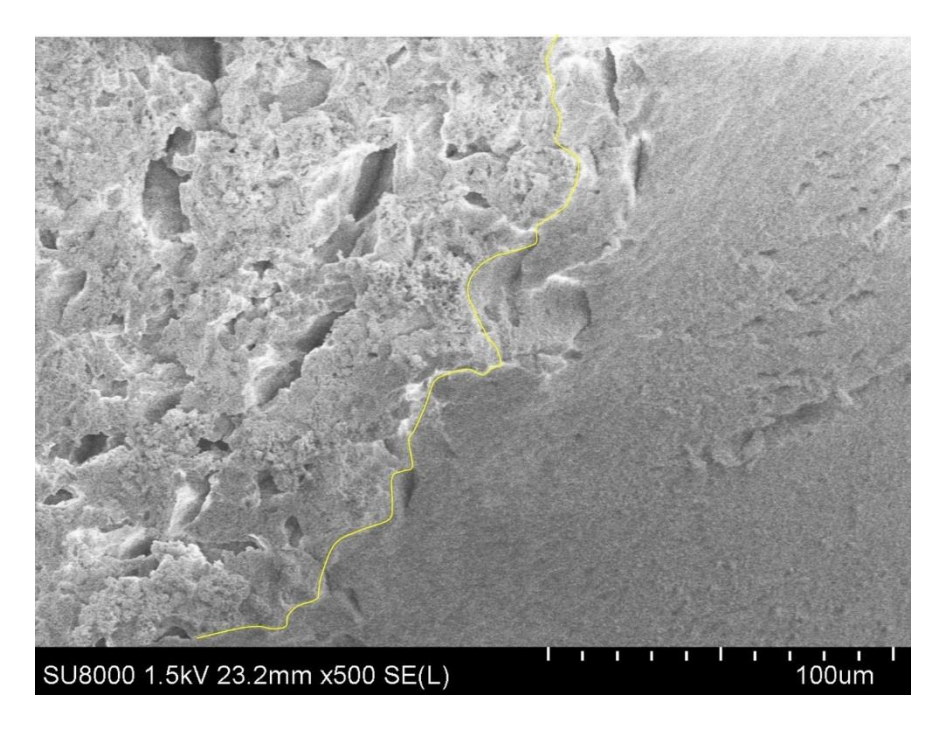


**Figure 18**: A fractured surface of the laser cut liner, allowing a view across its depth. The line denotes that right angled transition from the laser cut surface to the fractured surface. Any signs of densification was limited to the inner most 3um or so.

The structure of the aerogel is seen to be normal past a few microns into the layer, so densification does not penetrate beyond two to three microns at the surface. Evidently, the significant roughness of the surface results in a thicker dark band at the inner surface when viewed axially through the full length of the liner, as was the case in the X-ray cross-section image in Figure 17b.

## Effect of pulse length

Though the implication from Figure 18 is that the densification does not penetrate too far into the liner for this to be a concern, we investigated the impact of using a picosecond pulse laser. It is well known that lowering the pulse width to pico or femtosecond time-scales reduces the spread of the heat into the surface being cut<sup>11, 14</sup>. Of course, our other main quest was to look for any improvements in the blistered appearance of the surface. As seen in Figure 19, cursory trails using standard conditions did not show any significant difference compared to the results from a nano-second pulse laser seen in Figure 16. There was evidence of some surface glazing at the 45 mg/cc scale, and essentially none at 20mg/cc. In neither case was there any significant improvement in the surface quality.

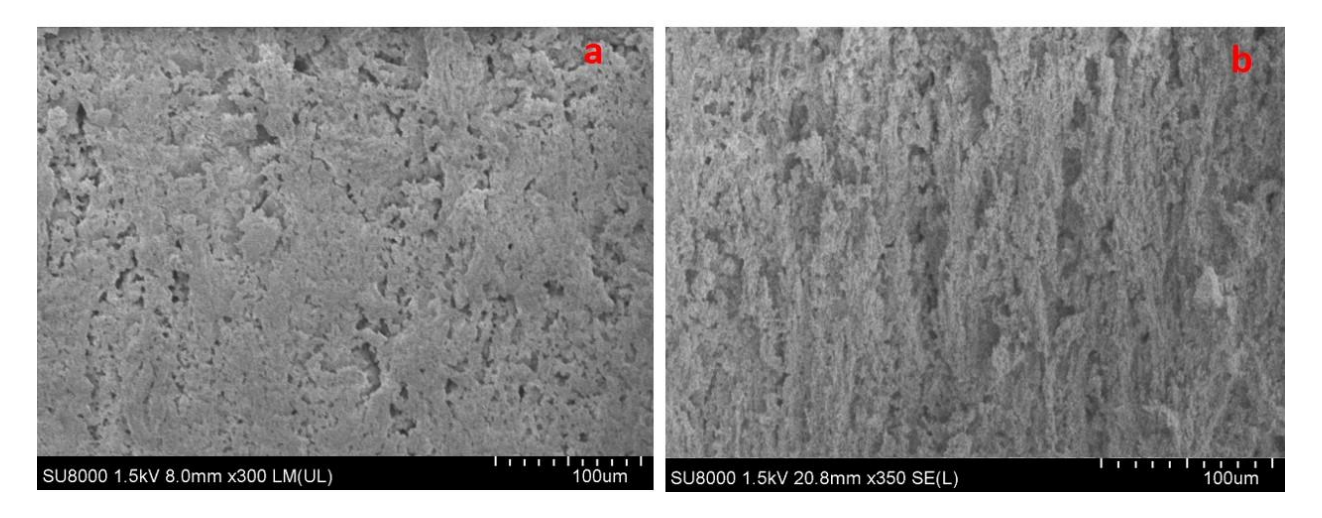


**Figure 19**: Surface topography for a 45 mg/cc (a) and 20 mg/cc (b) cut using a 355nm picosecond laser. Overall, these images look similar to the ones seen in Figure 16 with a nanosecond pulse.

# Effect of laser wavelength and average power:

For effective ablation, the preferred laser wavelength is one which is well absorbed by the material for the machined so that light energy can be efficiently converted to heat<sup>10, 14</sup>. Often in practice, the main limitation becomes the availability of high power lasers in the desired wavelength band, so practical ablation processes need to account for the drawback of fractional absorption by increasing the power delivered. In our case, tantala is mostly transparent over a wavelength range of 250nm to over 2.5um<sup>15</sup>, so optimizing for absorption is not an easy option. Results seen in Figures 16 and 17 were both with UV lasers, so we decided to investigate the effect of using a 1064nm IR laser (Keyence Laser Marker). Highlights of these results are seen in Figure 20. Note that the minimum power needed to cut the aerogel was considerably greater than that for the UV wavelength lasers mentioned above.

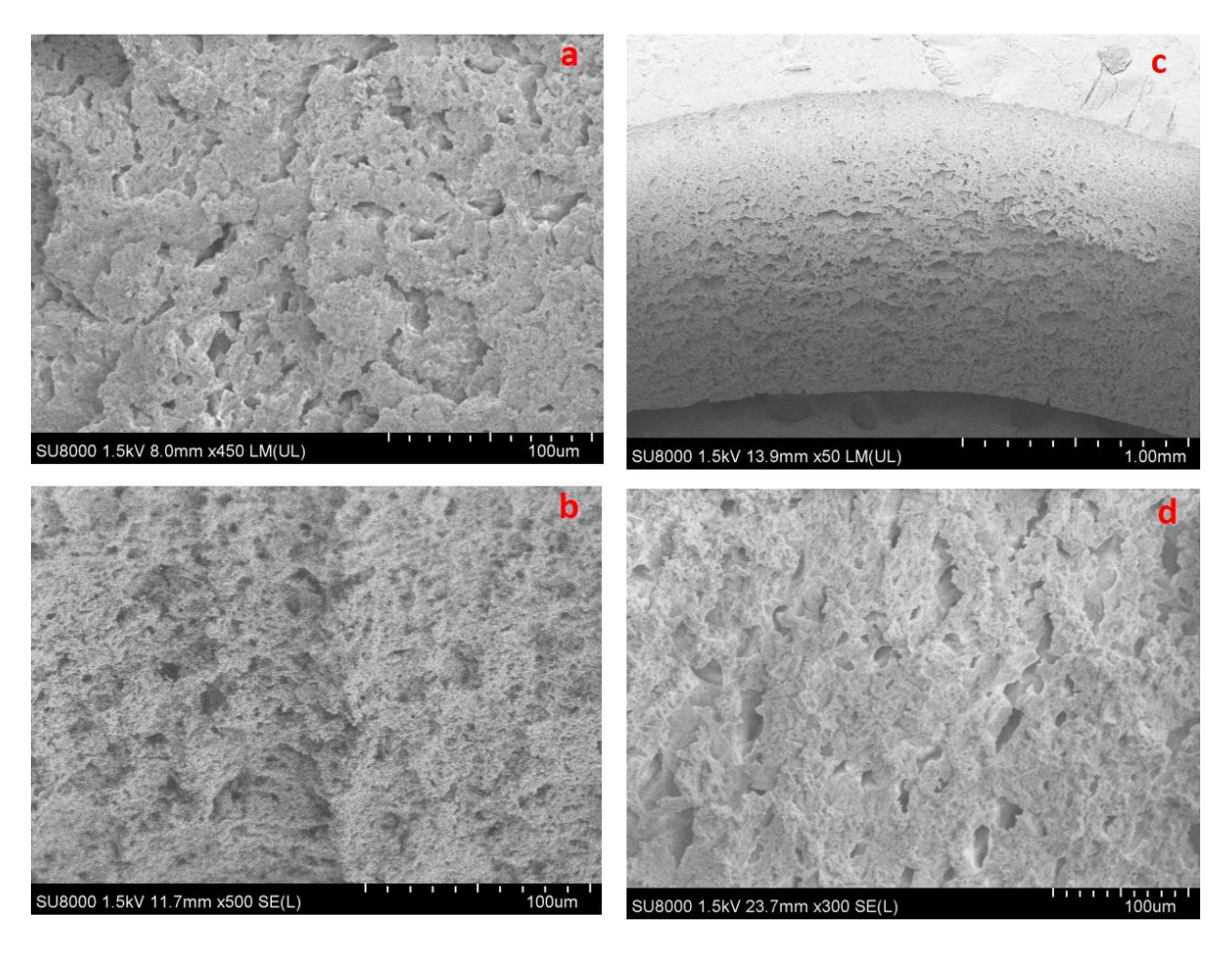


**Figure 20**: Surface topography for a 45 mg/cc (a) and 20 mg/cc (b) cut using a 1064nm nanosecond laser at 1.3W. Images in (c) and (d) are for surfaces cut at 0.65W. Again, these images have the same features as each other as well as those seen in Figure 16 and 19.

Again, there were telltale signs of surface melting both in the 45 and the 20 mg/cc foams at 1.3W but, as seen in Figure 20b, not at 0.65W, which was the threshold power needed to cut through. One other feature that stood out as a difference is the absence of the axial striations (Figure 20c). That was a persistent characteristic of all the cuts made with the 266nm Avia laser but was consistently absent when using the 1064 Keyence laser. Despite these subtle differences, the overall surfaces from the IR laser cuts resembled ones seen in our earlier efforts and the foam was prone to chipping.

### **Effect of repetition rate**

Interestingly, the biggest difference in surface quality came from varying the repetition rate (reprate). Using the 266 nm laser, changing the rep-rate from 1 to 30 kHz gave us cut surfaces that look like the ones seen in Figure 21. The cavity and fissure rich texture that was the staple of the previous samples was completely gone. Some vertical striations were still visible but only

marginally after the first 500um from top of the 2.5mm deep cut. The bulk of the surface resembled the one seen in Figure 19b, where the pitting was reproducibly non-existent. This surface was again seen to be independent of the power used- from 9 to 200 mW. It did however require more circular passes (15 or more) of the laser for the core to drop out. This represents an important advance for making better liners.

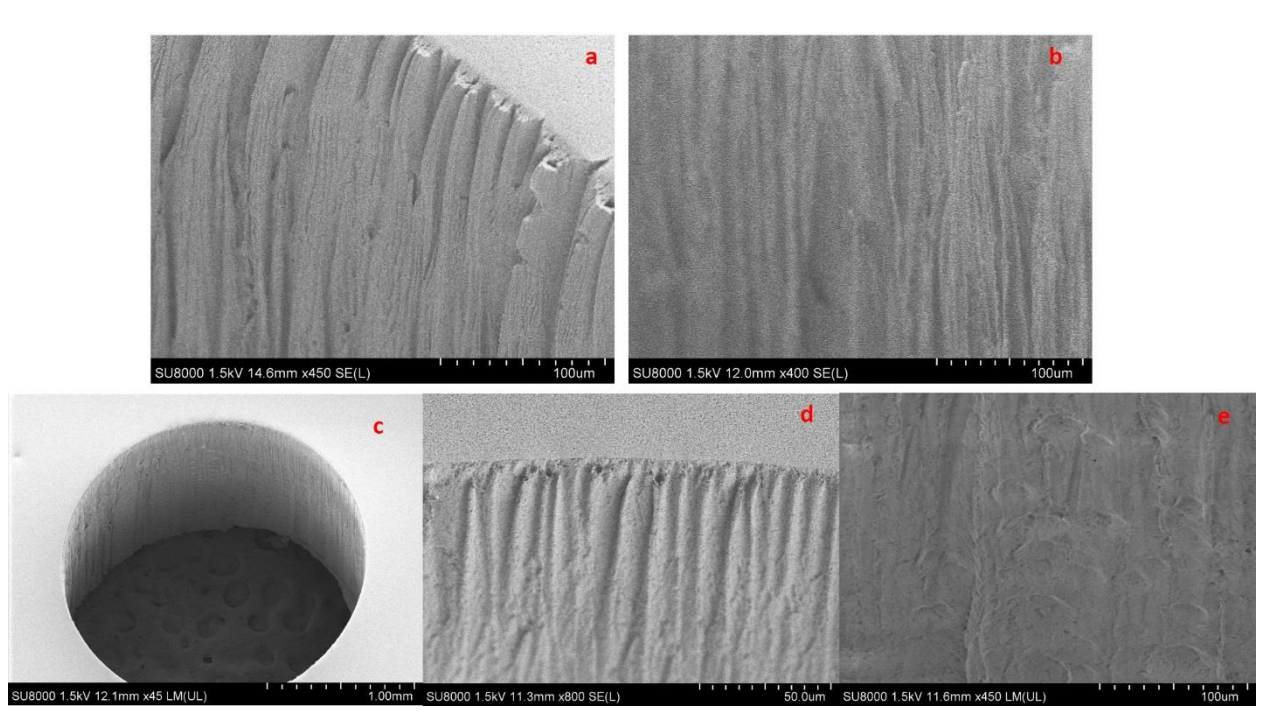


**Figure 21**: Remarkably different and smoother surface features seen from cuts using the 266nm laser but at 30KHz as opposed to the 1kHz for the baseline process. Images (a) and (b) are for 20 mg/cc foam whereas was images (c), (d) and (e) are for 10 mg/cc, both of which are remarkably similar in their absence of large pores and cuts. Images (a) and (d) are for the top portion of the foam while (b) and (e) are representative of the midsection or the bottom section along the liner depth. These show some difference in the manner in which the cutting progresses. However, neither is troublesome from a requirements standpoint.

Modeling of the physics of interaction of the foam lined hohlraum with the laser points to the need for densities as low as 10 mg/cc for obtaining the best performance. To that end, we extended these studies done at 45 or 20 mg/cc to 10 mg/cc. These results, seen in Figure 21c-e, show that the benefits seen at the higher densities are preserved at 10mg/cc as well. To really appreciate the implication of working with this density, we need to convert it to the equivalent solid fraction which is 1E-3, an astonishingly low number which constitutes an extremely delicate aerogel. We are in the process of confirming the reliability of the process in giving us a significant reduction in chipping and spalling as well as particle generation upon shaking.

Curiously, raising the rep-rate does not universally give us these advantages. Figure 20d is an example where going from a baseline rep-rate of 10kHz to 80kHz while using the 1064nm laser

(instead of the 266nm) made no noticeable difference in surface quality. It serves as a cautionary example for not drawing general mechanistic inferences too quickly. Doing a full scoping study to understand these phenomena was outside the purview of this work, so we cannot elaborate further on these intriguing trends.

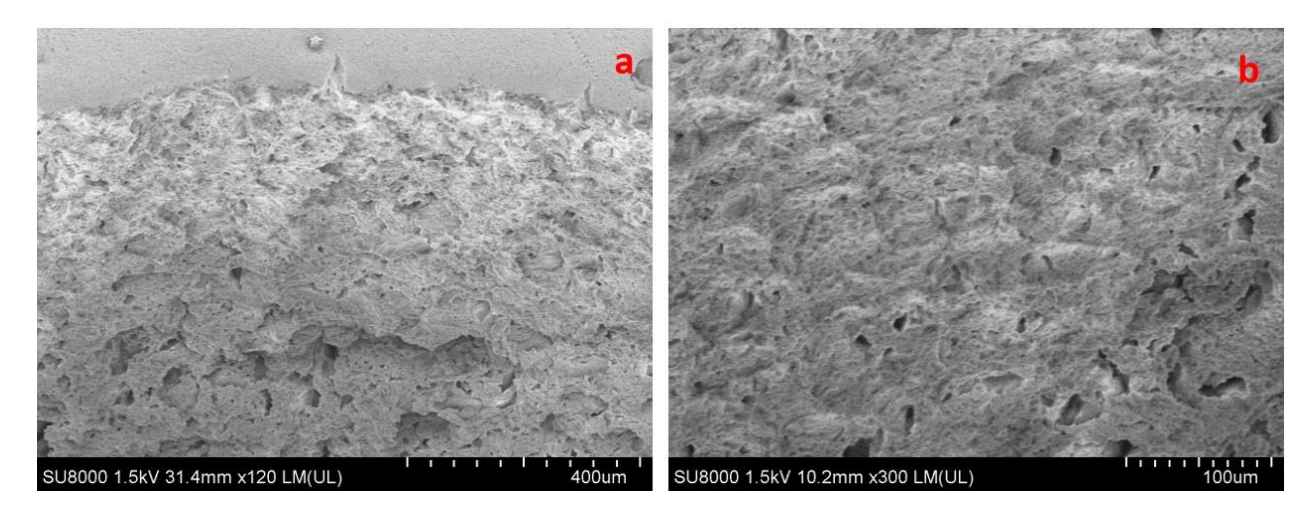


**Figure 22**: Images showing lack of change when we used a higher rep-rate (80kHz vs the earlier 10kHz) with the 1064nm nano-second laser. The lower magnification image (a) clearly shows the pits that happen to be less prominent in image (b). The stark contrast between the changes seen in Figure 21 and the lack of change seen here indicates that nature of the final surface is a result of a fairly complex interaction of the various laser cutting parameters.

## **Fabrication of foam-lined hohlraum targets**

To better understand the role of the foam in inhibiting wall motion, two types of targets were built. One type (Figure 23) is a simpler target where the ring is mounted on stalk with an underlying backlighter and second Ag strip on the side of the ring to generate a probe beam.

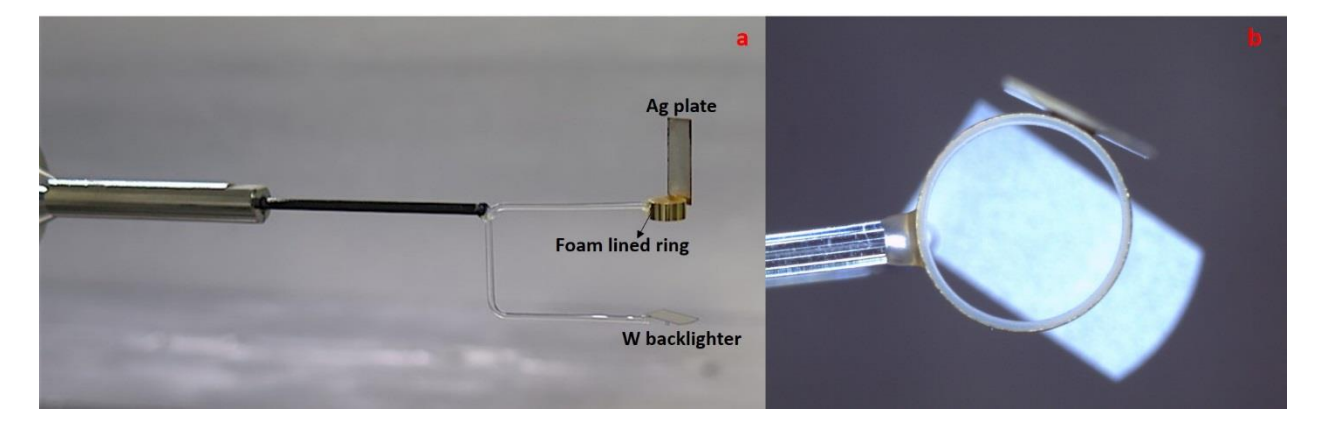


**Figure 23**: Simplified targets for exploring the role of the foam by seeking to directly visualize the motion of the hohlraum wall. Figure 23a is a side view of this design where we can see the tungsten backlighter underneath the ring and the Ag probe beam generator on the side. Top view image in (b) shows the liner inside the ring shortly before the target was shot.

The goal here was to avoid the painstaking assembly of a full-fledged cryogenic target and to be able to directly visualize the motion of the hohlraum wall. Initial results of this ongoing study have been very promising as they indicate that the liner does hold back the wall. More such targets are being conceived and built to systematically study the various foam properties.

In parallel, we seek to lay the groundwork for a campaign of shots using the NIF cryogenic target platform, starting with keyhole targets, followed by Symcaps before the ultimate DT layer shots. In Figure 24, we show as assembled 20mg/cc foam lined hohlraums inside the Al thermal-mechanical package (TMP) just prior to placement of the capsule.

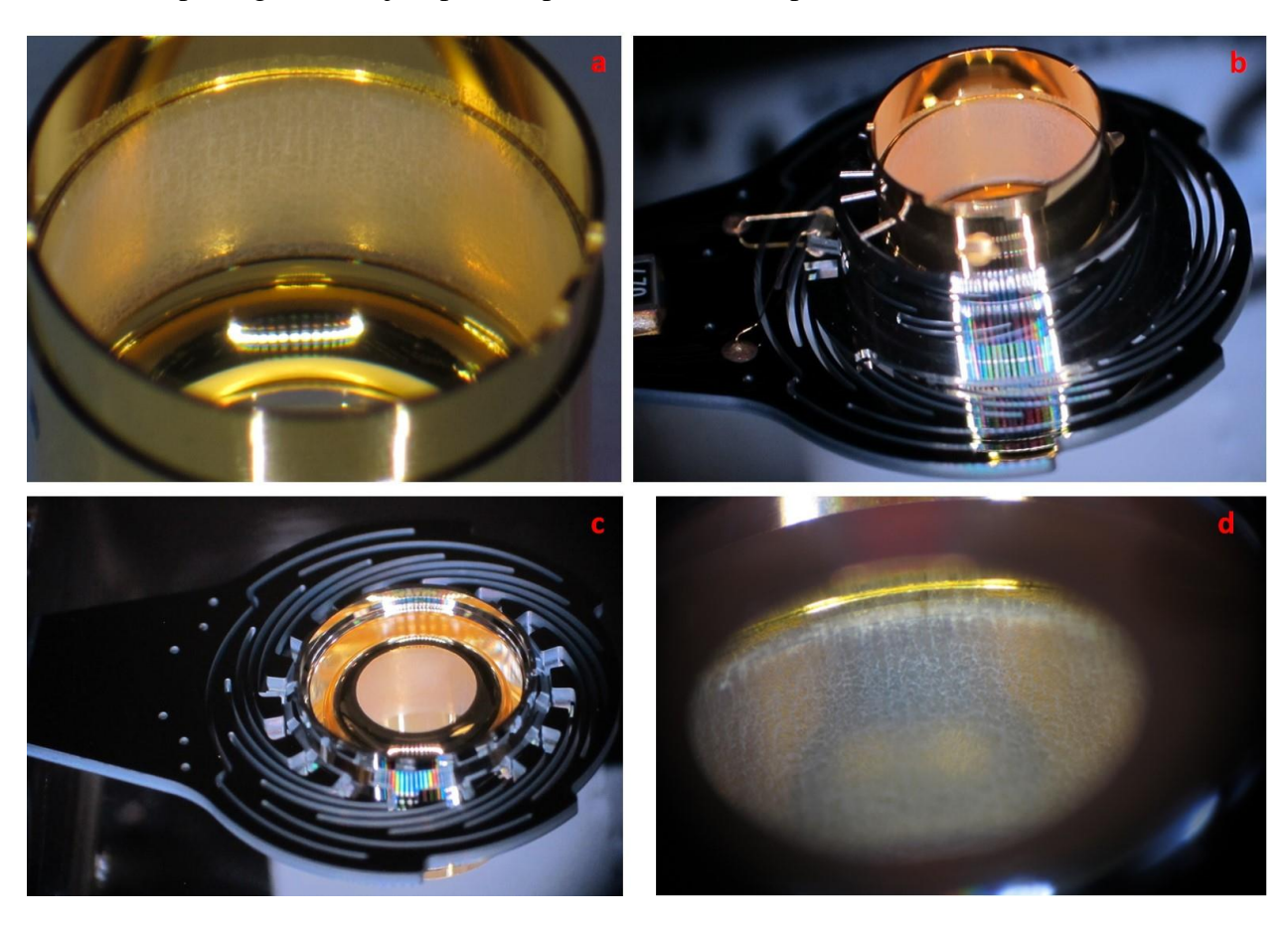


**Figure 24**: Images of the 20 mg/cc foam lined rings inside the TMP. The waist view (a and b) is used for comprehensive characterization of the foam while the LEH view (c and d) is the only option for checking the state of the liner before the target is sealed and fielded.

We need to visualize the foam liner at each of the step to ensure its integrity. In particular, once the target is assembled, the only view is through the LEH till the sealing window is put on as the last step. As seen in Figure 24, the full band of foam is in the line of sight and is distinct due to the diffused reflection from its surface. This illustrates the steady progress of this effort from early prototypes to target-worthy components with liner densities that were considered to be too low to be viable a short while ago.

#### **Summary**

In this paper, we have overviewed the evolution of foam liners for hohlraums which is seen a key step in opening up the design parameter space for enhanced hohlraum performance. Our current baseline process involves the use of tantala aerogel and a laser cutting process to shape it into a liner. We have described the optimizations that were needed to fulfill all the physics and fabrication requirements and provide a viable platform for building a growing number of foamliner based targets which seek experimental results that can be compared to simulations. Using a variety of processing advancements, foam liner density was lowered from initial 90 mg/cc to 10 mg/cc, with width varying from 200 to 500um and with low thickness variability. This has led to a number of successful foam lined hohlraum shots, both with and without the capsule. Early data from these exploratory shots is creating the necessary platform for a full-fledged campaign to understand and expand the role of the foams inside the hohlraum.

# Acknowledgement

We would like to thank John Hitchcock, Selim Elhadj and Nan Shen for their help with laser cutting. Thanks to Nathan Meezan and John Moody for their insight and guidance. Also, we thank Willie Hoke, Kelly Youngblood and Russell Wallace for making the ring targets and the entire target fabrication production team for the assembly of cryogenic targets.

This work was performed under the auspices of the US Department of Energy by Lawrence

Livermore National Laboratory under Contract DE-AC52-07NA27344 | LLNL-JRNL-736356

#### References

- 1. Edwards, M. J., et al, "The Ignition Physics Campaign on NIF: Status and Progress", J. Phys. Conf Ser., (688), 01201, p1-7, 2016
- 2. Moses, E.M., et al., "Ignition on the National Ignition Facility: a Path Towards Inertial Fusion Energy", Nucl. Fusion, 49, 1-9, 2009
- 3. Lindl, J. D., et al, "The Physics Basis of Ignition using Indirect-Drive Targets on the National Ignition Facility", Phys. Plasmas, 11(2), 340 (2004).
- 4. Meezan, N. B., et al, "Indirect Drive Ignition at the National Ignition Facility", Plasma Phys. Control. Fusion, 59, 014021, 2017
- Rosen, M. D., and Hammer, J. H, "Analytic Expressions for Optimal Inertial-Confinement-Fusion Hohlraum Wall Density and Wall Loss", Phys. Rev., 72, 056403, 2005
- 6. Zhang, L., et al., "Study on Optimal Inertial-Confinement-Fusion Hohlraum Wall Radial Density and Wall Loss", Phys. Plasmas., 18, 033301, 2011
- 7. Young, P. E., et al., "Demonstration of the Density Dependence of X-ray Flux in a Laser-Driven Hohlraum", Phys. Rev. Let., 101, 035001, 2008
- 8. Frederick, C. A., et al, "Fabrication of Ta2O5 Aerogel Targets for Radiation Transport Experiments Using Think Film Fabrication and Laser Processing", Fus. Sci. Tech., 55, 499, 2009
- 9. Hund, J. F., et al., "Silica, Metal Oxide and Doped Aerogel Development for Target Applications", Fus. Sci. Tech., 495, 669, 2006
- 10. Rihokova, L., and Chmelickova, H., "Laser Micromachining of Glass, Silicon and Ceramics, Adv. Mats. Sci. Eng., 2015, 584952, 2015
- 11. Bian, Q., et al., "Micromachining of Polyurea Aerogel Using Femtosecond Laser Pulses", J Non-Cryst Sol., 357, 186, 2011
- 12. Yalizay, B., et al., "Versatile Liquid-Core Optofluidic Waveguides Fabricated in Hydrophobic Silica Aerogels by Femtosecond-Laser Ablation", Opt. Mat., 47, 478, 2015
- 13. Sun, J., et al, "Ultrafast Laser Micromachining of Silica Aerogels", J Non-Cryst Sol., 281, 39, 2001
- 14. Shirk, M. D., and Molian, P. A., "A Review of Ultrashort Pulsed Laser Abalation of Materials", J. Laser Appl., 10, 18 1998
- 15. Franke, E., et al., "Dielectric function of Amorphous Tantalum Oxide from the Far Infrared to the Deep UV Spectral Region by Spectroscopic Ellipsometry", Faculty publications from the Department of Electrical Engineering at University of Nebraska, paper 17, 2000.